THE UNIVERSITY of EDINBURGH

Edinburgh Research Explorer

Pressure-Induced Jahn-Teller Switching in a Mn_{12} nanomagnet

Citation for published version:
Parois, P, Moggach, SA, Sanchez-Benitez, J, Kamenev, KV, Lennie, AR, Warren, JE, Brechin, EK, Parsons, S & Murrie, M 2010, 'Pressure-Induced Jahn-Teller Switching in a Mn_{12} nanomagnet', *Chemical Communications*, vol. 2010, no. 46, pp. 1881-1883. https://doi.org/10.1039/B923962F

Digital Object Identifier (DOI):
10.1039/B923962F

Link:
Link to publication record in Edinburgh Research Explorer

Document Version:
Publisher's PDF, also known as Version of record

Published In:
Chemical Communications

Publisher Rights Statement:
Publisher's Version/PDF: author can archive publisher's version/PDF

General rights
Copyright for the publications made accessible via the Edinburgh Research Explorer is retained by the author(s) and / or other copyright owners and it is a condition of accessing these publications that users recognise and abide by the legal requirements associated with these rights.

Take down policy
The University of Edinburgh has made every reasonable effort to ensure that Edinburgh Research Explorer content complies with UK legislation. If you believe that the public display of this file breaches copyright please contact openaccess@ed.ac.uk providing details, and we will remove access to the work immediately and investigate your claim.

Download date: 16. Mar. 2025

View Article Online / Journal Homepage / Table of Contents for this issue

Pressure-induced Jahn–Teller switching in a Mn_{12} nanomagnet†

Pascal Parois,[a] Stephen A. Moggach,[b] Javier Sanchez-Benitez,[b] Konstantin V. Kamenev,[b] Alistair R. Lennie,[c] John E. Warren,[c] Euan K. Brechin,[b] Simon Parsons*[b] and Mark Murrie*[a]

Received (in Cambridge, UK) 16th November 2009, Accepted 21st December 2009
First published as an Advance Article on the web 18th January 2010
DOI: 10.1039/b923962f

Published on 18 January 2010. Downloaded by University of Edinburgh on 29/05/2013 14:02:08.

Pressure-induced switching of a fast-relaxing single-molecule magnet to a slow-relaxing isomer is observed for the first time by using a combination of high pressure single-crystal X-ray diffraction and high pressure magnetic measurements.

The ability to control and increase magnetic anisotropy is one of the key targets in the development of single-molecule magnets (SMMs).[1] The prevalence of SMMs based on manganese ions is due to the large number of compounds that have been found to possess non-zero spin ground states, along with the large axial magnetic anisotropy of the Jahn–Teller distorted Mn(III) ion.[2] However, the effective energy barrier to reorientation of the magnetisation ($\Delta E/k_B$) in Mn(III)-based SMMs is highly sensitive to: the local symmetry of the molecule; the presence of low-lying spin states close to the ground state and perhaps most importantly, the spatial orientation of the elongated Jahn–Teller axes. The main contribution to the global anisotropy ($D_{cluster}$) arises from the tensor sum of the local single-ion axial anisotropy (D_i) of each Mn(III) centre. Mn_{12}acetate [$Mn_{12}O_{12}(OAc)_{16}(H_2O)_4$], the first and most studied SMM, consists of a ring of eight Mn(III) centres surrounding a central $Mn^{IV}{}_4O_4$ cube, bridged by oxide and acetate ligands.[2] There are two independent Mn(III) sites: the eight Jahn–Teller axes lie in near alignment with the magnetic easy axis, producing a $D_{cluster}$ of $-0.457(2)$ cm^{-1}.[3] In combination with the $S = 10$ spin ground state, this leads to an effective energy barrier of around 60 K.

There are many examples of Mn(III)-containing polynuclear complexes that are not SMMs, or are SMMs with only small energy barriers, due to the misalignment of the Jahn–Teller axes with the magnetic easy axis of the cluster.[4] Even bulk samples of Mn_{12}acetate contain a small portion of a so-called fast-relaxing (FR) Jahn–Teller isomer. This is a minority species, which displays faster relaxation than the majority species, or slow-relaxing (SR) isomer. These fast-relaxing isomers display a misaligned or 'horizontal' Jahn–Teller axis and a lower energy barrier of $\approx$ 40 K. The FR and SR isomers display different blocking temperatures and hence, differences in their magnetic properties.

High pressure has been used to study the static magnetic properties of Mn_{12}acetate at low temperature, suggesting that the blocking temperature decreases with pressure, there is some conversion of the SR to the FR isomer and quantum tunnelling is modified.[5] Inelastic neutron scattering measurements under pressure on Mn_{12}acetate also suggest conversion of a small portion of the sample from the SR to the FR isomer, and an increase in the axial anisotropy of both Mn_{12}acetate isomers with pressure.[6] However, there are no reported high pressure structural studies or high pressure dynamic magnetic measurements on Mn_{12}acetate or its derivatives. We have studied a fast-relaxing Mn_{12} isomer, $[Mn_{12}O_{12}(O_2CCH_2{}^tBu)_{16}(H_2O)_4]\cdot CH_2Cl_2\cdot MeNO_2$ (**1**), which displays a misaligned Jahn–Teller axis *i.e.* it exists as the 100% fast-relaxing species.[7] By using a combination of high pressure single-crystal X-ray diffraction and high pressure magnetic measurements we find that applied pressure switches the molecule reversibly from the 100% FR species to 100% SR species.

Compound **1** possesses a similar structure[7b] to Mn_{12}acetate. The peripheral ligation differs with $^tBuCH_2CO_2^-$ groups instead of acetate. Four H_2O ligands are also present, as in Mn_{12}acetate, though here two H_2O ligands are found on Mn12, forming the two Jahn–Teller elongated Mn–O bonds. The two remaining H_2O ligands are found on Mn10 and Mn6 atoms. Unlike Mn_{12}acetate, compound **1** has seven "vertical" Jahn–Teller bonds and one "horizontal" Jahn–Teller bond (Fig. 1 top) at 150 K. The horizontal Jahn–Teller bond is located on Mn8. At room temperature the Mn8–O distances span 1.930(4)–2.025(4) Å; the lack of a clear Jahn–Teller axis suggests disorder. The molecules interact *via* van der Waals interactions between ^{t}Bu groups.

On application of pressure, the main structural changes within the cluster occur at the Mn(III) centers. At 1.5 GPa, the Jahn–Teller elongated bonds on Mn5, Mn6 and Mn12 become more asymmetric, while those on Mn7 and Mn9–Mn11 all decrease by 0.02 Å on average. At Mn8 the Jahn–Teller elongated bond lengths decrease, and at 1.5 GPa the six Mn–O distances span the range 1.94(2) to 2.082(15) Å (see Table S1, ESI†), suggesting that the disorder present at ambient pressure persists. At 2.5 GPa, the behaviour of the elongated Jahn–Teller bonds at Mn8 is clearer. The horizontal Jahn–Teller bonds at ambient pressure switch to vertical Jahn–Teller bonds on Mn8–O14 and Mn8–O26 (Fig. 1 bottom). Between 1.5 and 2.5 GPa, most of the Jahn–Teller bonds on the remaining centres do not change significantly. Release of pressure re-establishes the coordination seen at ambient pressure.

[a] *WestCHEM, Department of Chemistry, University of Glasgow, University Avenue, Glasgow, UK G12 8QQ. E-mail: M.Murrie@chem.gla.ac.uk; Fax: +44 (0)141 330 4888*
[b] *School of Chemistry and Centre for Science at Extreme Conditions, University of Edinburgh, West Mains Road, Edinburgh, UK EH9 3JJ. E-mail: S.Parsons@ed.ac.uk*
[c] *STFC Daresbury Laboratory, Warrington, Cheshire, UK WA4 4AD*
† Electronic supplementary information (ESI) available: Crystal and ac data. CCDC 755025–755029. For ESI and crystallographic data in CIF or other electronic format see DOI: 10.1039/b923962f

Published on 18 January 2010. Downloaded by University of Edinburgh on 29/05/2013 14:02:08.

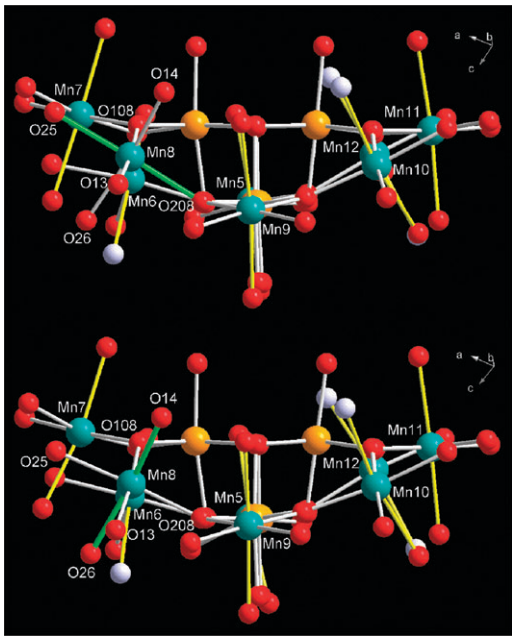

Fig. 1 The structure of the Mn–O core of **1** at ambient pressure (top) and at 2.5 GPa (bottom). The 'vertical' Jahn–Teller bonds are yellow and the Jahn–Teller bond on Mn8, which switches with applied pressure, is shown in pale green. [Mn(III), blue-green; Mn(IV), orange; O, red except H_2O ligands, lilac; for clarity, all C and H atoms are omitted]. At 2.5 GPa: Mn8–O108 1.88(3); Mn8–O13 1.89(3); Mn8–O208 1.90(3); Mn8–O25 2.03(3); Mn8–O14 2.105(17); Mn8–O26 2.19(2) Å.

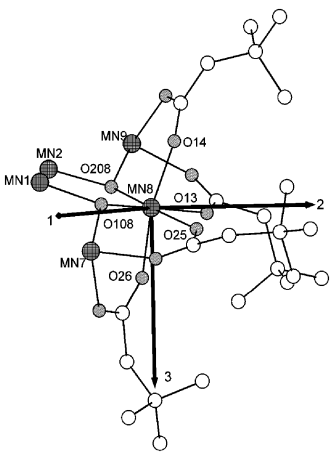

Fig. 2 Orientation of the principal components of the strain tensor superimposed on the coordination sphere of Mn8. The direction of the largest component of strain is labelled '1', and the smallest '3'.

The strain tensor expresses the overall effect of pressure on a crystal structure, revealing the directions which undergo the greatest and least compression. When the two largest components of strain are superimposed on Mn8 they are found to lie in the 'horizontal' plane containing the oxo-ligands, which is also the plane containing the Jahn–Teller axis at ambient pressure (Fig. 2). The effect of pressure is therefore to compress the local structure around Mn8 mostly in the horizontal direction, 'pushing' the Jahn–Teller axis into the normal vertical orientation. The new orientation of the Jahn–Teller axis also corresponds to the direction of the smallest strain component.

At ambient pressure the formula unit contains $MeNO_2$ and CH_2Cl_2 of solvation. At 1.5 GPa the occupancies of the solvent model best with a combined total of 1.25 molecules per formula unit; the solvent was removed altogether in modelling the 2.5 GPa dataset. Models of partially occupied solvent can be subject to reinterpretation even with fully complete diffraction data. At high pressure, where data are incomplete because of the pressure cell, the situation is yet more uncertain. However, the data suggest the solvent is released into the hydrostatic medium on compression, and reabsorbed on decompression (see Table S2, ESI†). Conversion from fast-relaxing to slow-relaxing Mn_{12} species can be affected by solvent loss,[7] and our high pressure data appear to be consistent with this theory.

The ac susceptibility of **1** was measured‡ from ambient pressure to 1.44 GPa and this also shows conversion from the fast-relaxing to the slow-relaxing species. The evolution of the out-of-phase signal as a function of pressure is shown in Fig. 3. The ambient pressure data reveal only one peak at low temperature (T_{max} = 2.1 K at 1 Hz) due to the fast-relaxing species. At 0.47 GPa the low temperature peak shifts to higher temperature (*ca.* 2.3 K) with a significant decrease in its intensity. At the same time a broader peak appears at around 4 K. Hence, at 0.47 GPa both the fast-relaxing and slow-relaxing species are present. This trend continues at 0.82 and 1.12 GPa. On reaching 1.44 GPa there is no low temperature peak, and only the high temperature peak is observed (T_{max} = 4.1 K at 1 Hz) due to the exclusive presence of the slow-relaxing species. The switch is reversible: after the pressure is released, the data again reveal only one peak at low temperature. The ac data are in excellent agreement with the single-crystal X-ray diffraction study, where we have shown that the molecule becomes 'more axial' with increasing pressure as the misaligned Jahn–Teller axis flips from horizontal to vertical. The pressure regime to see the full switch is slightly different between the two measurements, probably due to the diffraction study being carried out at ambient temperature whereas the magnetic study is carried out below 10 K.

The out-of-phase peak that arises from the FR species shifts to higher temperature with increasing pressure (Fig. 3). This is consistent with an increase in the effective energy barrier. An Arrhenius analysis of the frequency dependent ac data

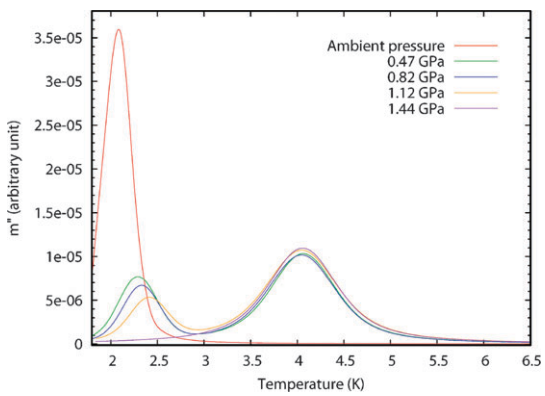

Fig. 3 Conversion of the fast-relaxing (FR) to the slow-relaxing (SR) species: evolution of the out-of-phase ac susceptibility for **1** under pressure, measured at a fixed frequency of 1 Hz.

This journal is © The Royal Society of Chemistry 2010

Published on 18 January 2010. Downloaded by University of Edinburgh on 29/05/2013 14:02:08.

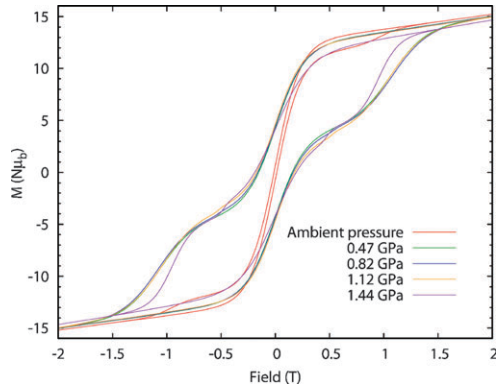

Fig. 4 Evolution of the hysteresis loops of **1** at 2 K, from ambient pressure to 1.44 GPa.

collected at each pressure was carried out. At ambient pressure, $\Delta E/k_B$ for the fast-relaxing species is 41 K, increasing to 46 K at 1.12 GPa. The relaxation time also increases from 4×10^{-10} s to 8×10^{-10} s. The ambient pressure values compare well to those reported ($\Delta E/k_B = 42$ K, $\tau_0 = 2.2 \times 10^{-10}$ s).[7] An increase in the effective energy barrier of the fast-relaxing species with pressure will be related to the change in molecular geometry. There could be an increase in the $D_{cluster}$ parameter or a decrease in the rhombic anisotropy parameter ($E_{cluster}$), as the molecule becomes more axial. High pressure HFEPR measurements would be needed to investigate this further.

At 0.47 GPa, the peak at *ca.* 4 K in the ac data is consistent with the presence of a pressure-induced slow-relaxing species (Fig. 3). The energy barrier of the pressure-induced SR species of **1** is 63 K, comparing well to the value of 62 K previously reported for the SR species $[Mn_{12}O_{12}(O_2CCH_2{}^tBu)_{16}(H_2O)_4]\cdot CH_2Cl_2\cdot MeCN$ (**2**).[8] From 0.47 GPa to 1.12 GPa, our data do not reveal any significant changes in the energy barrier or relaxation time for the pressure-induced slow-relaxing species of **1**.

The evolution of the hysteresis loop under pressure at 2 K is shown in Fig. 4. At ambient pressure, the hysteresis loop from the FR species has a small coercive field. Application of pressure starts to convert the sample to the SR species and the coercive field increases. This pressure-induced conversion from the FR species to the SR species seen in the ac data causes an increase in $\Delta E/k_B$ from *ca.* 40 K to *ca.* 60 K. Therefore, the hysteresis loop should widen under pressure because as $\Delta E/k_B$ increases, the blocking temperature (T_B) also increases. The ac data at 1.44 GPa show full conversion to the SR species. We have used the steps in the hysteresis loop at 1.44 GPa to estimate the axial anisotropy of the pressure-induced SR species of **1** as $D = -0.61$ K, which is in excellent agreement with the D parameter obtained from single-crystal low temperature hysteresis loops for the SR species **2**.[8]

In conclusion, we have shown for the first time, using high pressure diffraction and magnetic data, that conversion of fast-relaxing to slow-relaxing Mn_{12} species occurs by flipping the misaligned Jahn–Teller axis, producing a pure pressure-induced slow-relaxing isomer.

We thank the EPSRC for financial support and the STFC for provision of synchrotron beam-time.

Notes and references

‡ Single crystals of **1** were prepared as in ref. 7 and authenticated using single-crystal diffraction at ambient pressure and 150 K. High pressure diffraction data were collected with synchrotron radiation on a Bruker APEX II diffractometer at the SRS on Station 9.8 ($\lambda = 0.4780$ Å). Data collection and processing procedures followed ref. 9. Two crystals were studied. For the first, data were collected at 1.5 and 2.5 GPa; for the second, data were collected at ambient pressure, 1.5 GPa and then at ambient pressure again. During refinement (SHELXL)[10] similarity restraints were applied to all $^tBuCH_2CO_2^-$ ligands; the ^{t}Bu groups were also restrained to be locally three-fold symmetric. For the ambient pressure datasets (which were collected with the sample on a fibre) one solvent molecule of CH_2Cl_2 was treated using the van der Sluis–Spek method.[11] This is not possible for the high pressure datasets because they suffer from low completeness as the result of shading by the body of the pressure cell, and both solvent molecules were modelled explicitly at 1.5 GPa; they appear to be essentially absent at 2.5 GPa. Thermal motion is generally high, particularly in the $CH_2{}^tBu$ moieties, several of which are disordered. Only Mn and O atoms were refined with anisotropic displacement parameters. Conventional *R*-factors for the ambient pressure datasets are 0.0809 and 0.0817; those for the high pressure datasets are 0.1083 (1.5 GPa) and 0.1102 (2.5 GPa). These values are reasonable given the relatively modest level of modelling that is possible with incomplete data. A table of crystal data and further refinement details is available in the ESI.† CCDC reference numbers 755025–755029. The magnetic data were measured using a Quantum Design MPMS XL SQUID magnetometer. The datasets from ambient pressure to 1.12 GPa were collected in a CuBe pressure cell. The final dataset at 1.44 GPa was collected in a NiCrAl pressure cell, as the maximum pressure of the CuBe cell had been reached. A small chip of lead was used as a pressure calibrant. Several block-shaped single crystals (total mass 4.84 mg) of **1** were placed in the Teflon capsule along with Daphne 7373 (IDEMITSU-ILS) oil in order to have a hydrostatic pressure. The sample was aligned by field cooling in a field of 5 T from ambient temperature to 10 K.

1 (*a*) D. Gatteschi and L. Sorace, *J. Solid State Chem.*, 2001, **159**, 253; (*b*) H. Oshio and M. Nakano, *Chem.–Eur. J.*, 2005, **11**, 5178; (*c*) J. Ribas-Arino, T. Baruah and M. R. Pederson, *J. Am. Chem. Soc.*, 2006, **128**, 9497; (*d*) R. Inglis, L. F. Jones, G. Karotsis, A. Collins, S. Parsons, S. P. Perlepes, W. Wernsdorfer and E. K. Brechin, *Chem. Commun.*, 2008, 5924; (*e*) J. Cirera, E. Ruiz, S. Alvarez, F. Neese and J. Kortus, *Chem.–Eur. J.*, 2009, **15**, 4078.

2 (*a*) R. Bagai and G. Christou, *Chem. Soc. Rev.*, 2009, **38**, 1011; (*b*) A. J. Tasiopoulos and S. P. Perlepes, *Dalton Trans.*, 2008, 5537.

3 I. Mirebeau, M. Hennion, H. Casalta, H. Andres, H. U. Güdel, A. V. Irodova and A. Caneschi, *Phys. Rev. Lett.*, 1999, **83**, 628.

4 (*a*) A. Ferguson, K. Thomson, A. Parkin, P. Cooper, C. J. Milios, E. K. Brechin and M. Murrie, *Dalton Trans.*, 2007, 728; (*b*) A. M. Ako, I. J. Hewitt, V. Mereacre, R. Clérac, W. Wernsdorfer, C. E. Anson and A. K. Powell, *Angew. Chem., Int. Ed.*, 2006, **45**, 4926.

5 (*a*) G. G. Levchenko, E. E. Zubov, V. N. Varyukhin, A. B. Gaspar and J. Real, *J. Phys. Chem. B*, 2004, **108**, 16664; (*b*) Y. Suzuki, K. Takeda and K. Awaga, *Phys. Rev. B*, 2003, **67**, 132402.

6 A. Sieber, R. Bircher, O. Waldmann, G. Carver, G. Chaboussant, H. Mutka and H. U. Güdel, *Angew. Chem., Int. Ed.*, 2005, **44**, 4239.

7 (*a*) M. Soler, W. Wernsdorfer, Z. Sun, J. C. Huffman, D. N. Hendrickson and G. Christou, *Chem. Commun.*, 2003, 2672; (*b*) Z. Sun, D. Ruiz, D. N. Hendrickson, N. R. Dilley, M. B. Maple, M. Soler, K. Folting, G. Christou and J. Ribas, *Chem. Commun.*, 1999, 1973.

8 M. Soler, W. Wernsdorfer, Z. Sun, D. Ruiz, J. C. Huffman, D. N. Hendrickson and G. Christou, *Polyhedron*, 2003, **22**, 1783.

9 A. Dawson, D. R. Allan, S. Parsons and M. Ruf, *J. Appl. Crystallogr.*, 2004, **37**, 410.

10 G. M. Sheldrick, *SHELXL*, University of Gottingen, Germany, 2003.

11 P. V. d. Sluis, *Acta Crystallogr., Sect. A*, 1990, **46**, 194.